Electroconvective Instability with a Stabilizing Temperature Gradient
II. Experimental Results

Robert J. Turnbull

CSR TR-68-4 February, 1968

CENTER FOR SPACE RESEARCH
MASSACHUSETTS INSTITUTE OF TECHNOLOGY

Electroconvective Instability with a Stabilizing Temperature Gradient
II. Experimental Results

Robert J. Turnbull

CSR TR-68-4 February, 1968

ELECTROCONVECTIVE INSTABILITY WITH A STABILIZING TEMPERATURE GRADIENT II. EXPERIMENTAL RESULTS

Abstract

A uniform vertical electric field produces an instability in a poorly-conducting fluid subject to a vertical temperature gradient. A previous paper[1] presents the theory for this instability. Here measurements are made of the voltage at the threshold for instability. Since the instability occurs as an overstability, the frequency at the threshold was also measured. These results are in agreement with those predicted by the theory. Heat transfer experiments show a significant increase in heat flow under the influence of the electric field.

I. INTRODUCTION

Reference 1 contains a theoretical derivation of the condition for the electric field instability of a fluid with a stabilizing temperature gradient. This paper presents the results of experiments performed to test that theory. Three different sets of experiments were performed. First measurements of the voltage and frequency for instability were made. Next the unstable modes were excited electrically. Finally the increase in heat transfer due to the electric field was measured.

The increase in heat transfer which is observed when electric fields are applied to a fluid has been investigated by several researchers. Using cylindrical geometry the increase was measured in polar gases by Senftleben[2-6] and co-workers. Kronig and Schwarz[7] introduced a similarity theory which allowed a quantitative interpretation of Senftleben's data. This similarity theory provided correlation for data from liquids using both a.c.[8,9,10] and d.c.[11-12] fields. There has been some controversy over the relative merits of a.c. and d.c. fields with comparison made by Allen[13] and Coulson and Porter.[14] Allen[13] obtained an inhibition of heat transfer using d.c. fields, but offers no valid explanation. Coulson and Porter had enhancement of heat transfer with both a.c. and d.c. fields, but the d.c. fields produced a stronger effect. They concluded that free charge effects must be important. Gross and Porter,[15] performing experiments similar to those of this paper, observed electroconvection with d.c. fields but none with the same strength a.c. field. These last two papers[14,15] give results consistent with those presented here.

II. MEASUREMENT OF THE THRESHOLD VOLTAGE AND FREQUENCY

A. Experimental Apparatus

The basic experimental apparatus is shown in Figure 1. It consists of a rectangular test tank made of glass walls with aluminum top and bottom which serve as electrodes. In contact with the upper electrode is a container with a metal bottom. This container is filled with oil which is maintained at a constant high temperature. The lower electrode rests on a large aluminum plate which is partially immersed in water at room temperature. In this manner, a constant temperature gradient is maintained across the experiment. The test tank is completely filled with fluid so that no free surfaces exist. A high-voltage d.c. power supply is used to provide the vertical electric field which produces the instability. The onset of motion is detected visually by means of a Schlieren or a shadowgraph apparatus.

B. Description of the Instability

When no electric field is applied to the fluid, the image cast by the Schlieren system with a horizontal knife edge is light on the top and dark on the bottom, with a sharp transition line in between. This is shown in Figure 2a. The fluid and image are, of course, stationary. In this case the image should be uniformly lit according to the principles of operation of the Schlieren apparatus, but the imperfections of our apparatus give the image shown. This is not serious, since the optical system is used only to detect the fluid

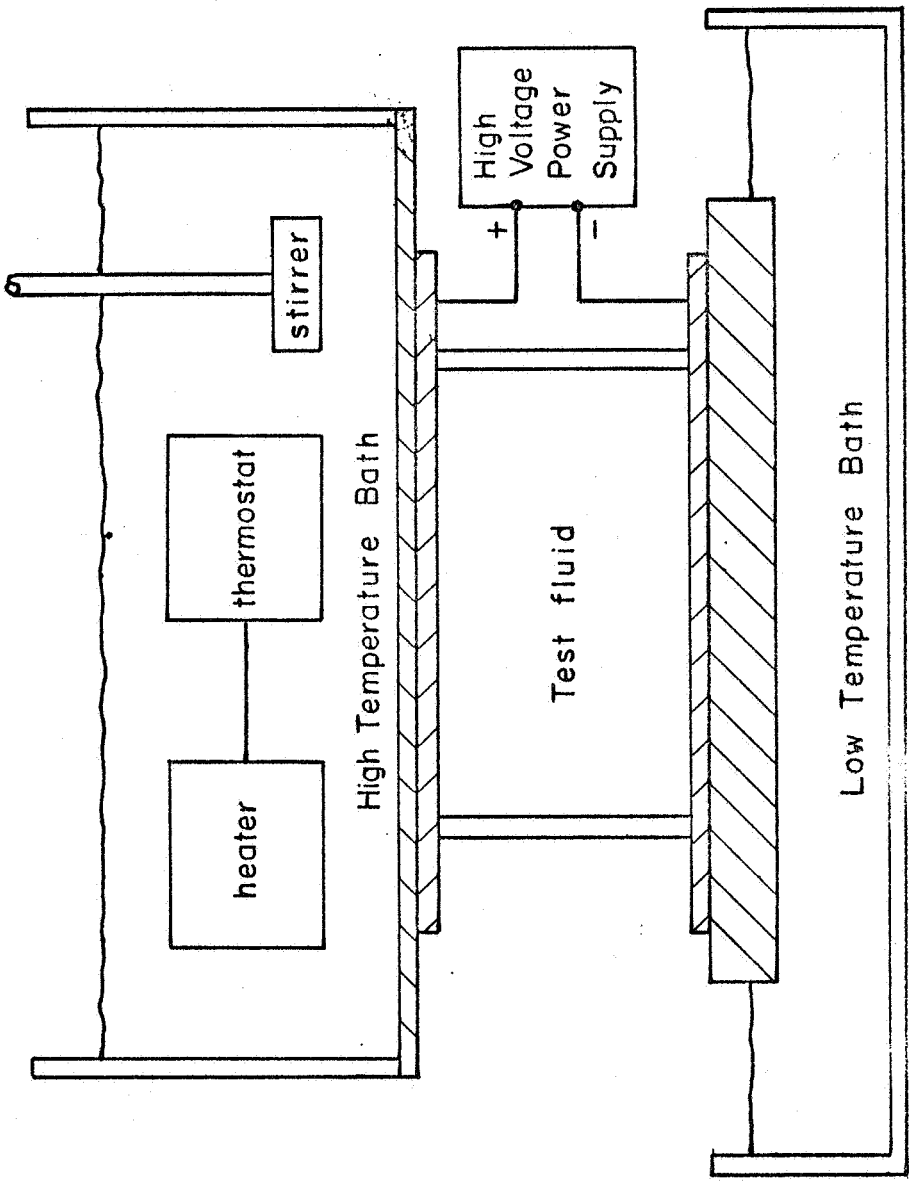

Fig. 1 Experimental Apparatus

motions, and not to measure the temperature gradient.

When an electric field of less than the threshold value for convection is applied, the transition from light to dark occurs along a crinkled surface, as in Figure 2b. Also, dark spots sometimes appear in the light region. The entire fluid is motionless except for occasional local movement around the dark spots. A possible explanation for this motion is that it is caused by the non-uniformity of the fluid. There is nothing in the theoretical model[1] which accounts for either the crinkles or the local motion.

As the voltage is raised, a threshold is reached at which the fluid begins to move, at first very slowly and then faster. This is the threshold for instability predicted by the theory. The images cast by the optical systems show that the waves in the tank are moving downward. The theory predicts that all the unstable modes will have phases which travel downward. If the voltage is maintained a nonlinear state is reached which has a regular pattern. The Schlieren image of the nonlinear state, Figure 2c, shows light and dark stripes at an angle with the vertical traveling in a direction perpendicular to themselves from hot to cold. Again, this is consistent with the theory. There seems to be a tendency for these stripes to start at the walls of the tank, move toward the center, and then break up when they collide with those moving in from the opposite wall. In a shadowgraph image the stripes are replaced by narrow bright lines. A sequence of shadowgraph pictures taken five seconds apart is shown in Figure 3, where

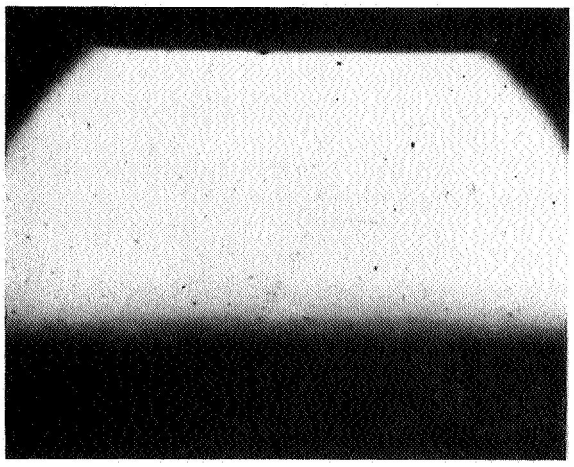

(a.) NO VOLTAGE.

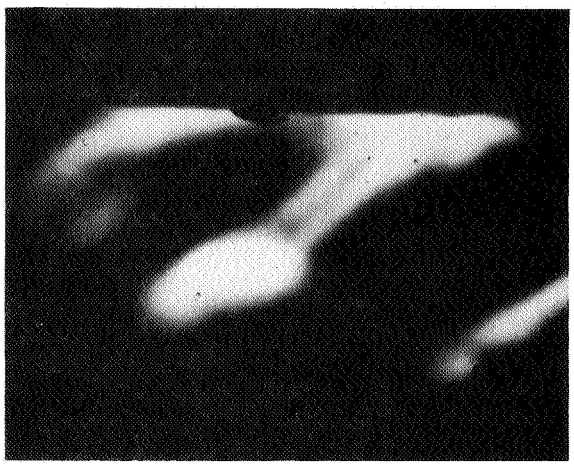

(c.) VOLTAGE AT THRESHOLD.

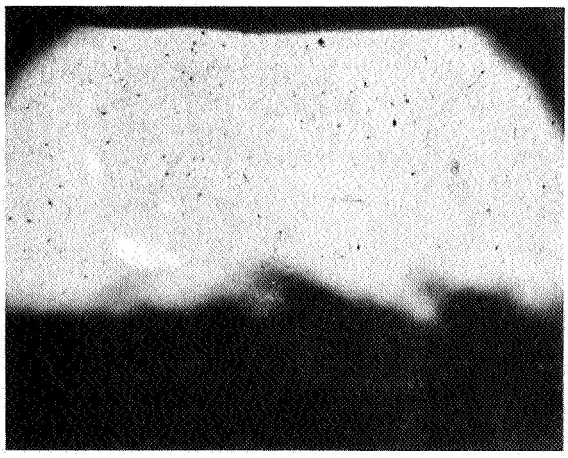

(b.) VOLTAGE BELOW THRESHOLD.

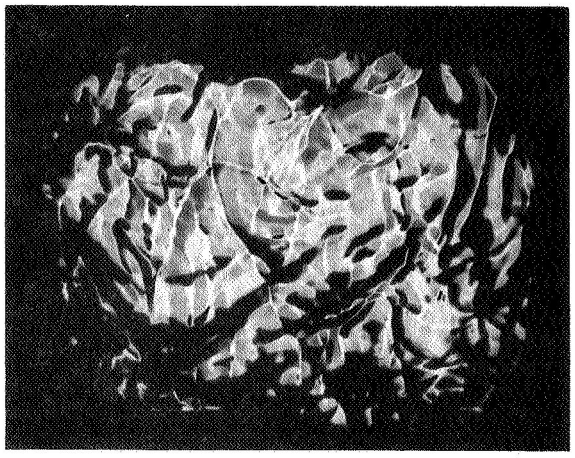

(d.) VOLTAGE TWICE THRESHOLD VALUE.

Fig. 2 Schlieren Pictures of the Instability

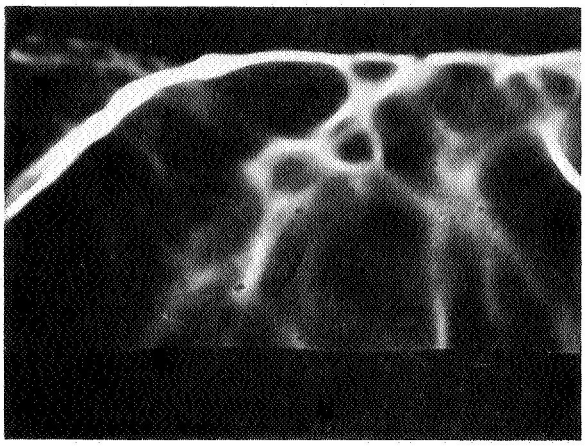

(1)

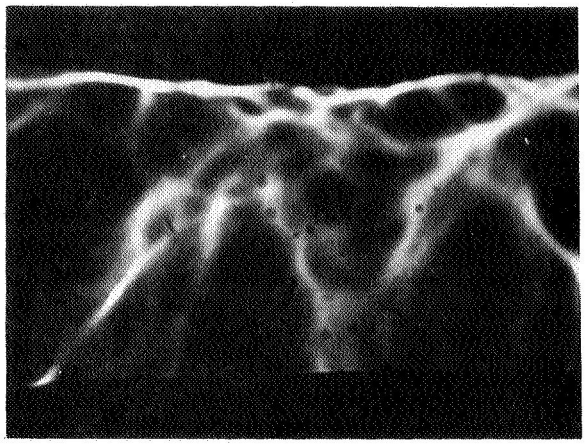

(3)

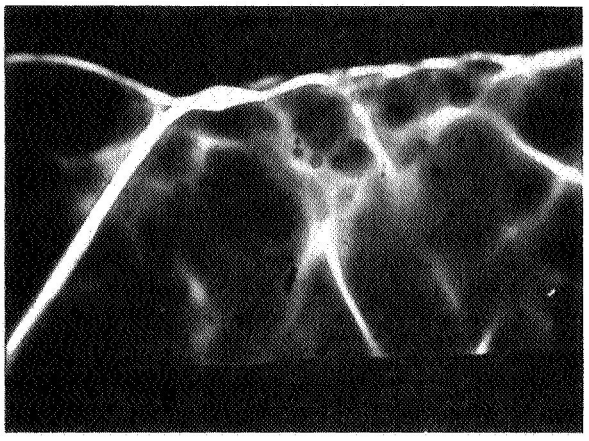

(2)

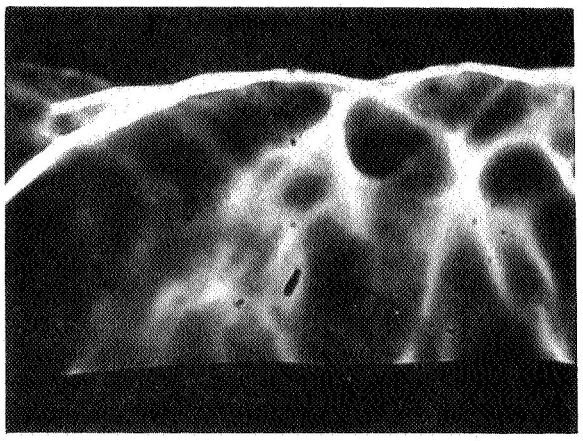

(4)

Fig. 3 Shadowgraph pictures showing the moving phases. The pictures were taken five seconds apart. The bright line in the upper left hand corner of picture (1) moves down and to the right and then breaks up in picture (3). Picture (4) is very similar to picture (1) showing that the waves have a period of about 15 sec.

the movement of these lines can be seen. These lines tend to have a periodicity in both space and time over a local region of the tank. The shadowgraph image shows that, instead of varying sinusoidally in space, as was assumed in Reference 1, the perturbations form sharp discontinuities (the bright lines).

In order to view the motion of the fluid, sawdust particles were inserted into the flow. The fluid moves parallel to the lines of constant phase. The shadowgraph image shows that the direction of the velocity reverses whenever one of the bright lines pass. This is shown in Figure 4 which consists of a sequence of pictures taken two seconds apart. The particle indicated by the arrow rises in a direction tangential to the bright line until it passes and then descends afterward.

Raising the voltage well above the threshold causes the fluid to become very turbulent, as shown in Figure 2d. The Schlieren image soon becomes all light, indicating that the convection has destroyed the temperature gradient. After the temperature gradient has been destroyed the motion decreases in intensity, but the system is still quite turbulent.

C. Voltage Data and Correlation with Theory

The apparatus of Figure 1 was used to measure the threshold voltage. Two fluids were used: corn oil and castor oil, and data was taken for two different tank sizes and several temperature gradients. The experimental data is shown as dots with error brackets in Figures 5-8 along

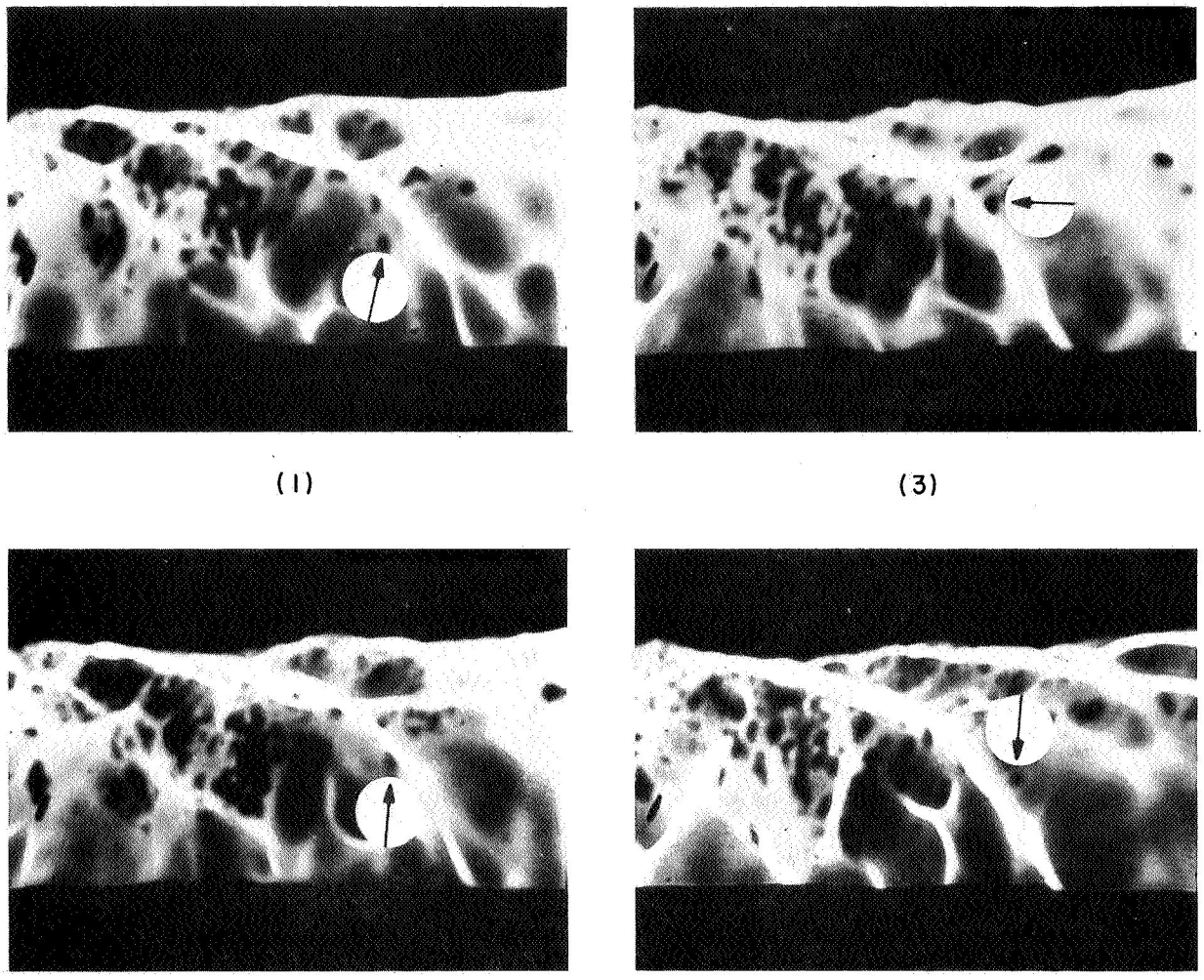

Fig. 4 Fluid motions illustrated by a particle placed in the corn oil. The particle indicated by the arrow rises between pictures (1) and (2) before the wave front (bright line) passes. After the wave front has passed, the particle goes down (pictures 3 and 4). The pictures were taken two seconds apart.

Fig. 5 Voltage for instability for corn oil in a one-inch high tank as a function of the temperature difference. The bottom is maintained at 25° C. The lines are theoretical curves with the dots and error brackets experimental data. The theoretical curves are calculated using the equations of reference 1.

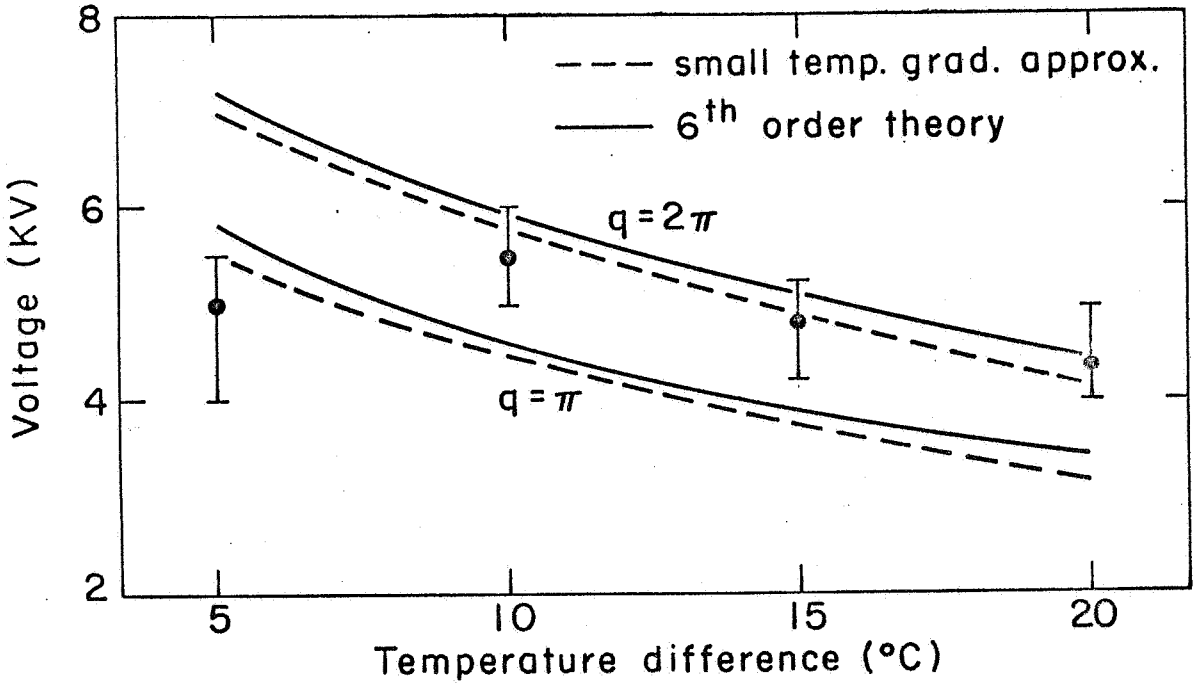

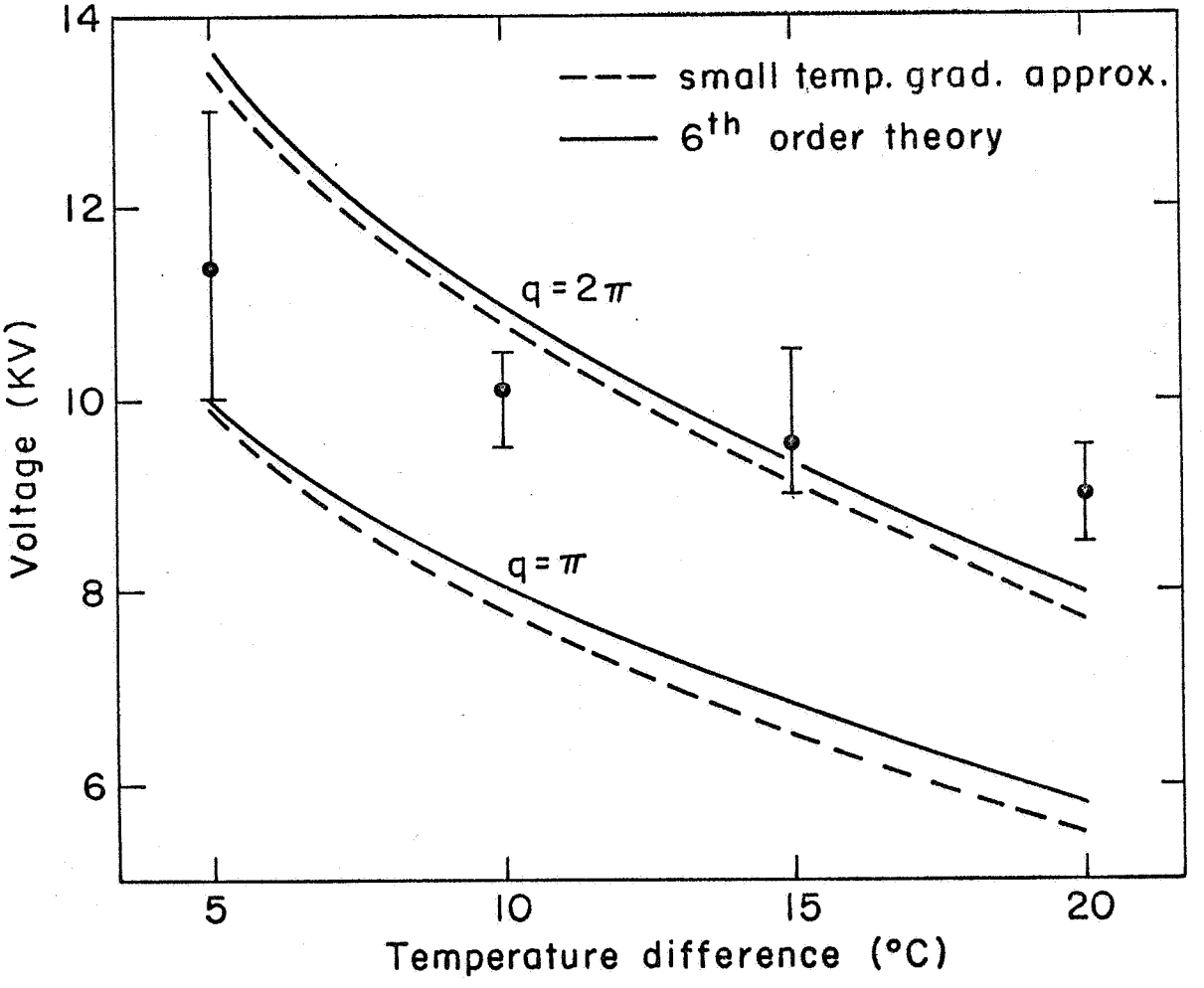

Fig. 6 Voltage for instability for corn oil in a two-inch high tank. The bottom is maintained at 20°C.

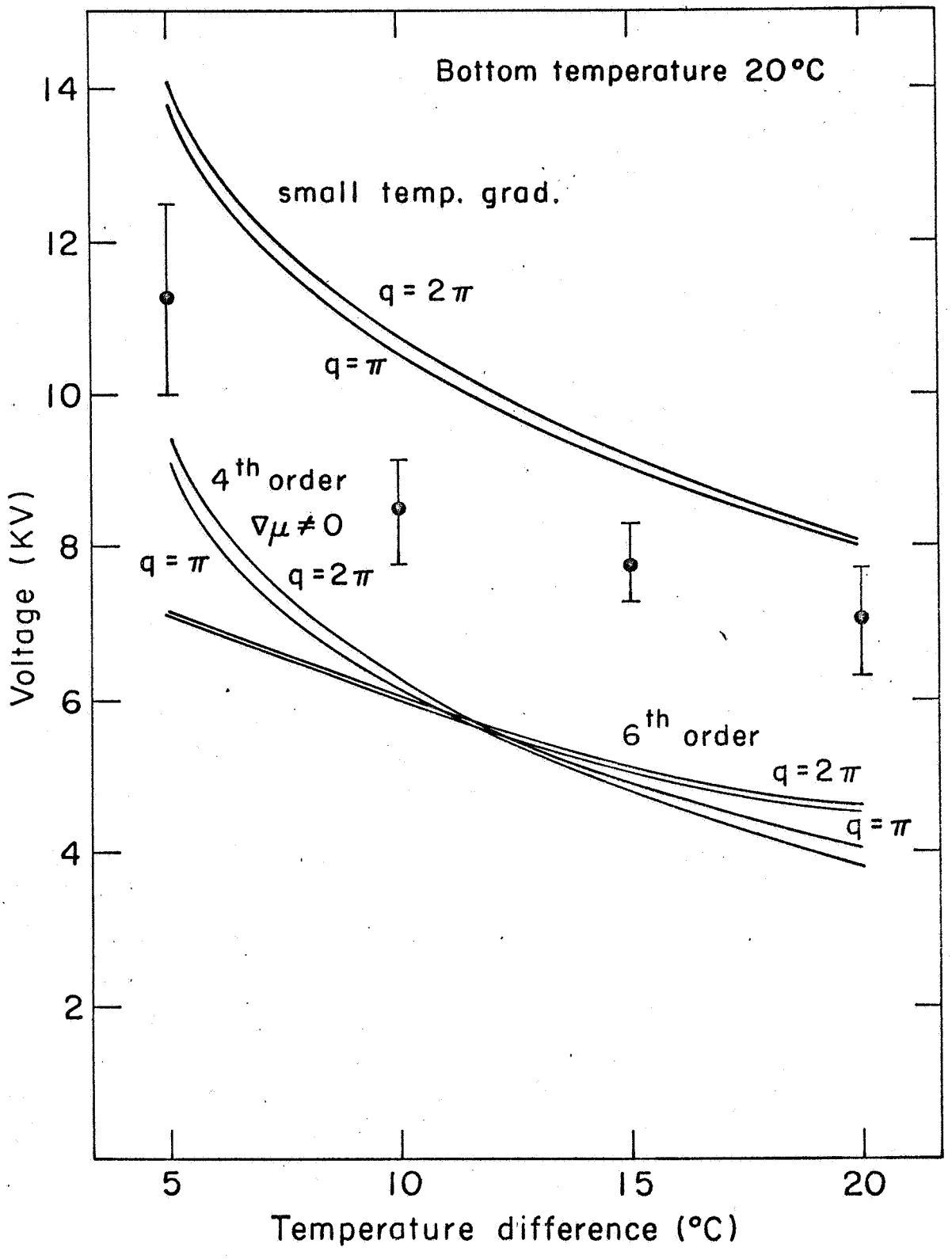

Fig. 7 Voltage for instability for castor oil in a one-inch high tank. The bottom is maintained at 20° C.

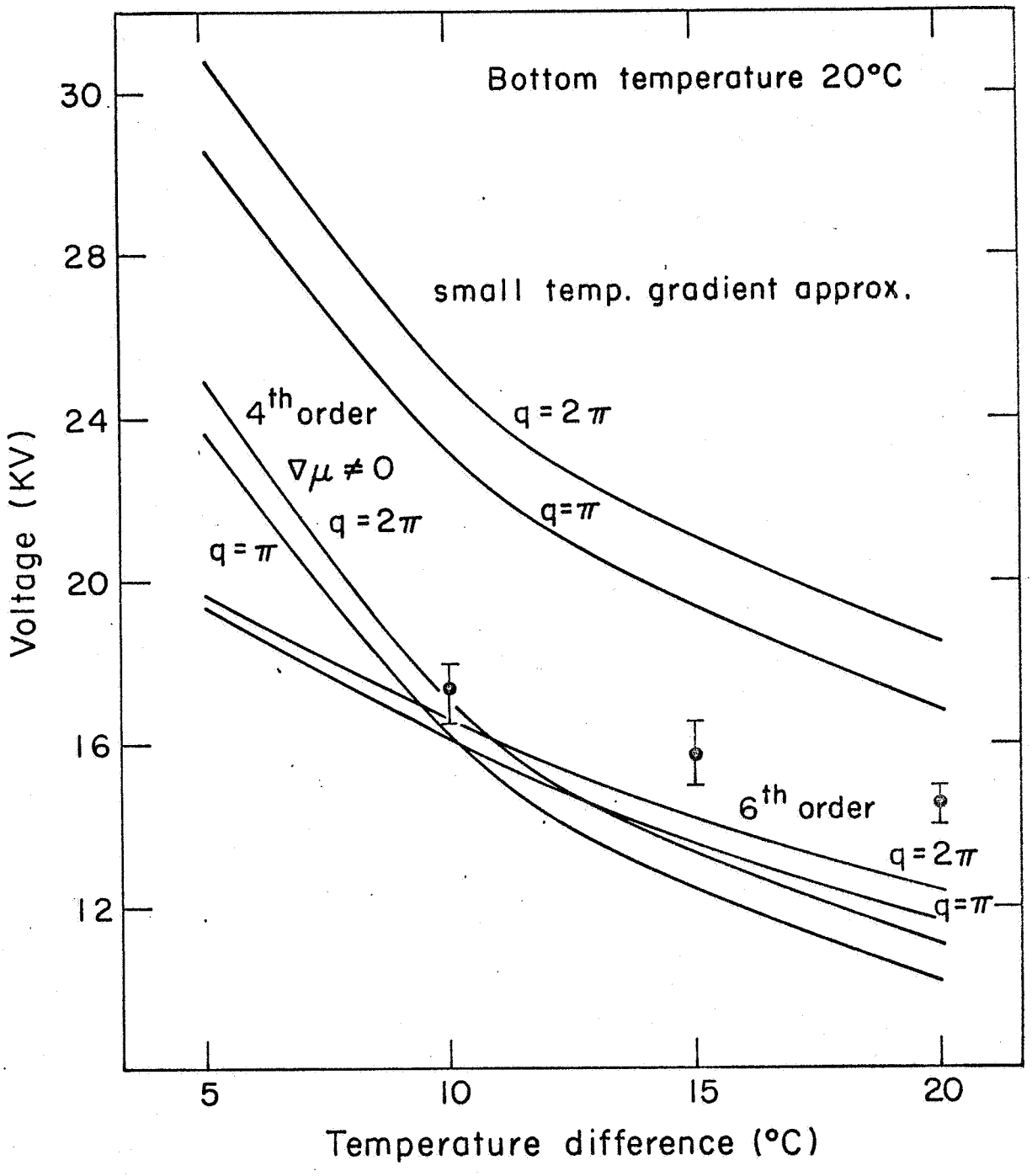

Fig. 8 Voltage for instability for castor oil in a two-inch high tank with a bottom temperature of 20° C.

with theoretical curves. The theoretical curves are drawn using the data in Figure 9 and Table 1.

The four theoretical lines in Figures 5 and 6 result from calculations both with and without the small temperature gradient approximation and with vertical wavenumbers equal to π and 2π.[16] The small temperature gradient approximation is valid for these situations since it produces results similar to those obtained without the approximation. The experimental results correlate with the curves for a vertical wavenumber of 2π indicating that this is approximately the wavenumber for the first unstable mode. The data for a temperature difference of 5^{o} C is unreliable, possibly because for that case the temperature gradient effects may be of the same order of magnitude as other effects not considered. (Electroconvection occurs in fluids with no temperature gradient for reasons which require further investigation.)

Figures 7 and 8 show the data for castor oil. In these figures there are six theoretical curves. The added curves are drawn from calculations using the small temperature gradient approximations but including $\nabla\mu$. Here, the small temperature gradient approximation is poor unless the gradient in viscosity is taken into account. The correlation is not as good as for corn oil. Possible reasons for this are:

1) The "Boussinesq approximations" are not as valid because of the great variations in the viscosity.

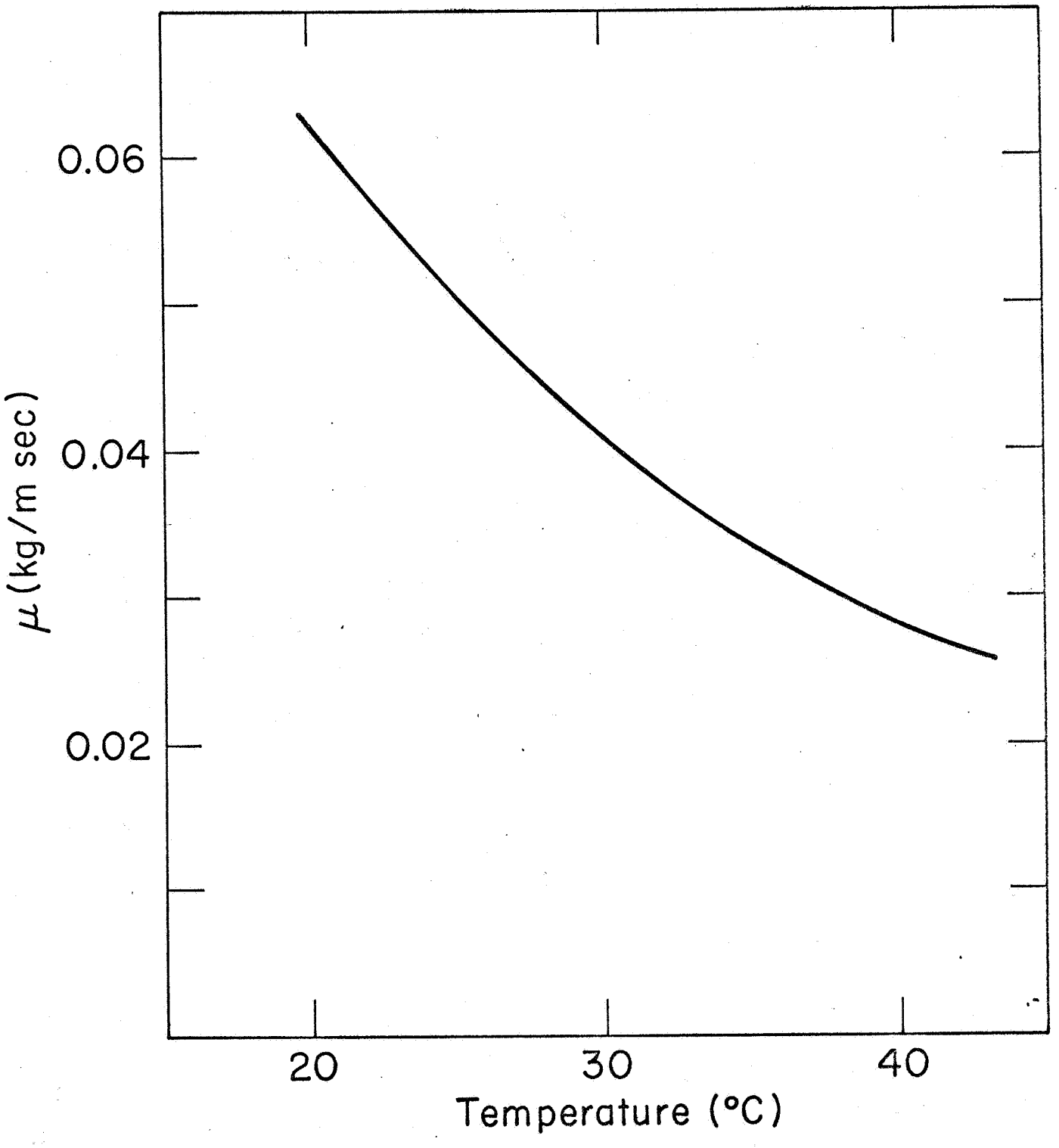

Fig. 9 Fluid properties as functions of temperature: a) Viscosity of corn oil

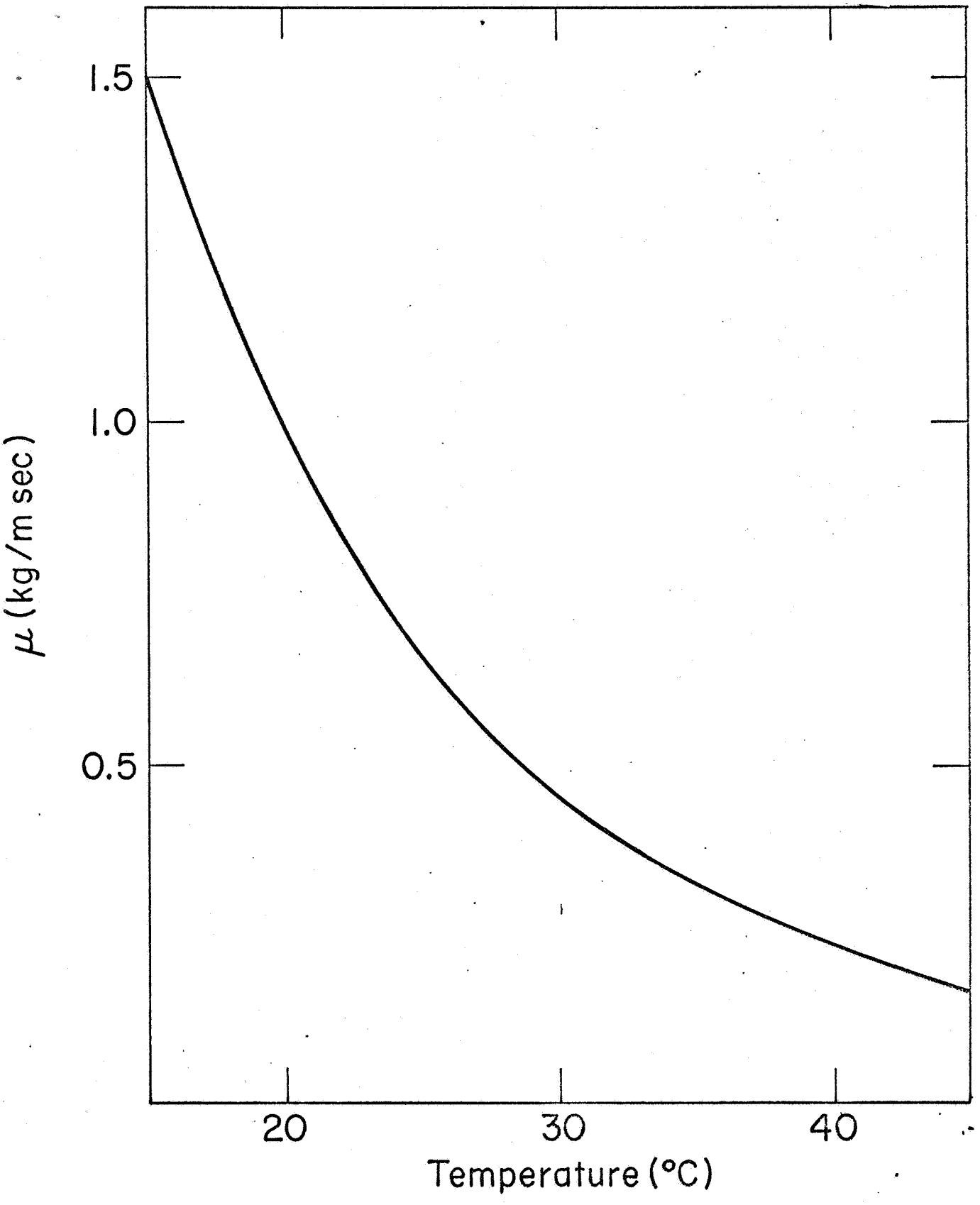

Fig. 9 Fluid properties as functions of temperature: b) Viscosity of castor oil

Fig. 9 Fluid properties as functions of temperature: c) Conductivity of corn oil

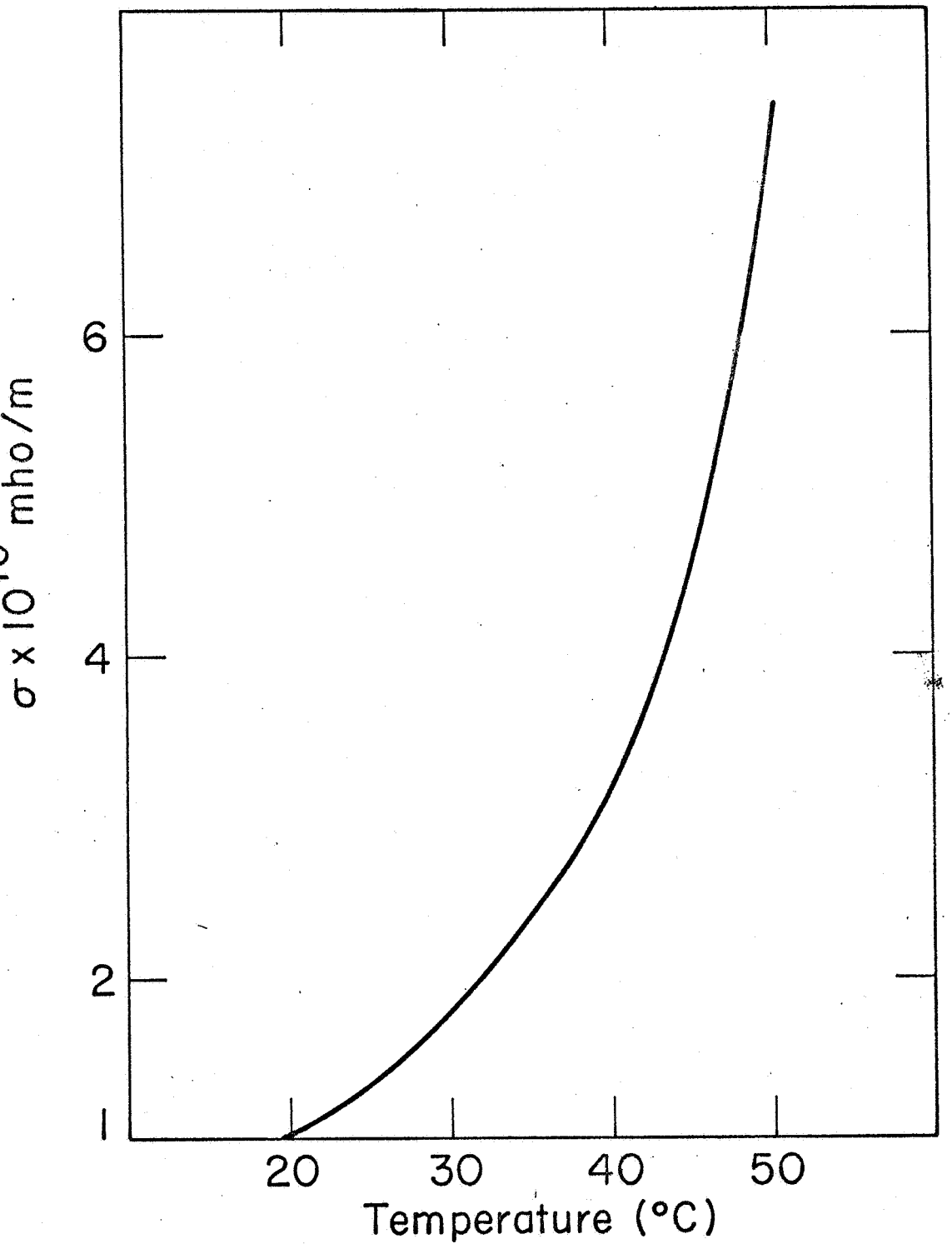

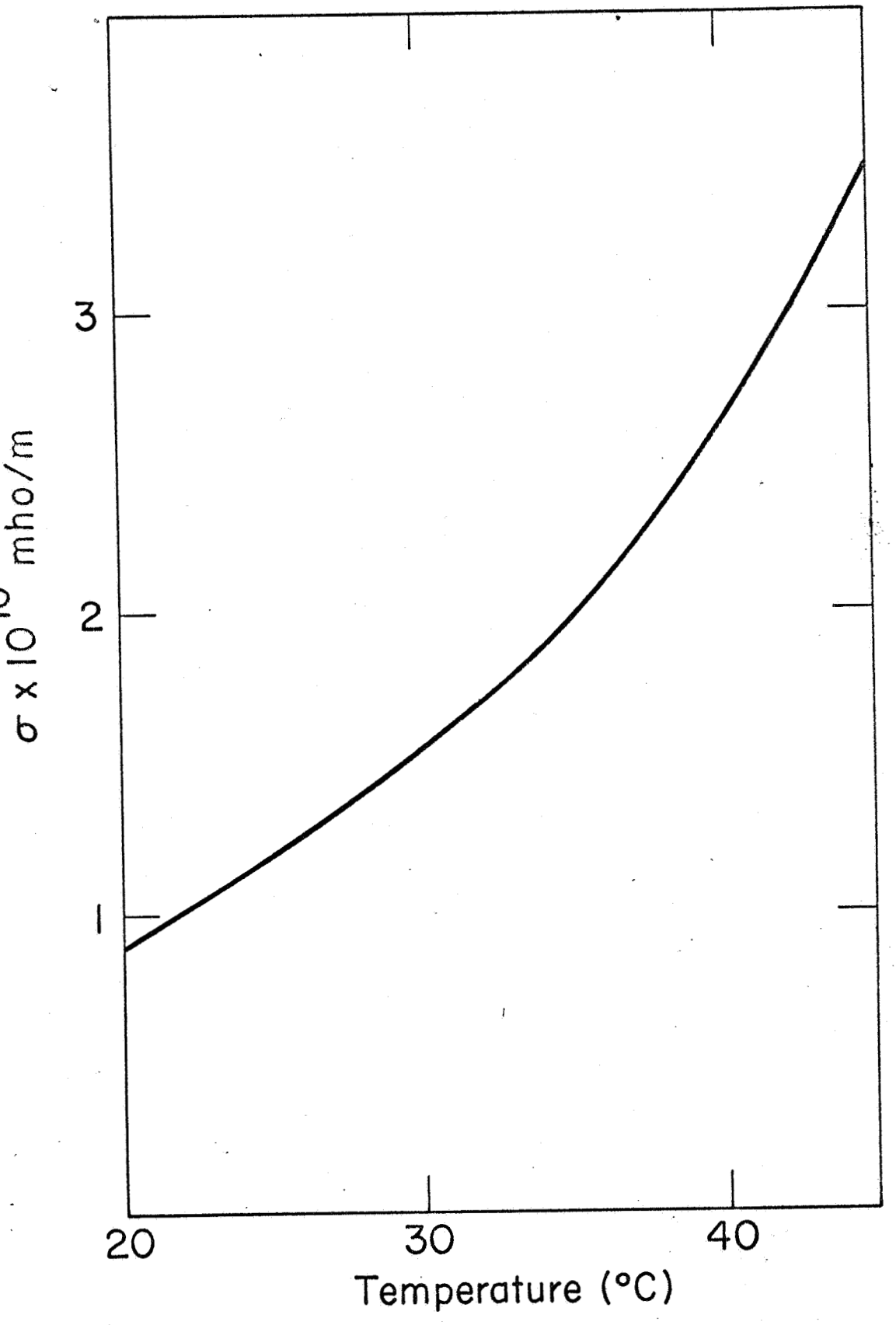

Fig. 9 Fluid properties as functions of temperature: d) Conductivity of castor oil

Table 1

Corn Oil

$\rho = .914$ kg/m^3 at 30° C

$\frac{1}{\rho}\frac{d\rho}{dT} = .00066^\circ C^{-1}$.

$\epsilon = 3.1 \epsilon_o$

Castor Oil

$\rho = 960.3$ kg/m^3 at 20° C

$\frac{1}{\rho}\frac{d\rho}{dT} = .00072^\circ C^{-1}$

$\epsilon = 4.67 \epsilon_o$

2) For a very viscous fluid the growth rate for the instability increases very slowly with the voltage. Thus the threshold could be passed before motion was detected.

D. Frequency Measurements

In order to measure the frequency at the threshold, a pinhole was cut in the screen on which the Schlieren image was projected. Behind the pinhole was a phototube whose output was connected to a strip recorder. The frequency was read off the recordings. The frequency data is shown in Figure 10 along with the theoretical predictions using a vertical wavenumber of 2π and a horizontal one of at least π. Since the agreement between theory and experiment is not as good as that for the voltage experiments, it was decided to check the frequency with another experiment. In this experiment the voltage was set at a value slightly below threshold and the waves were excited by a sinusoidal source. The resonant frequency was then measured. The excitation was accomplished by placing a small perfectly conducting plate just below and parallel to the upper electrode. The small plate was then excited by a low frequency voltage and the resultant fluid motion observed.

If the d.c. voltage was 1 kv or more below the threshold value, the driving signal caused a small response whose amplitude varied little with frequency. When the d.c. voltage was just below the

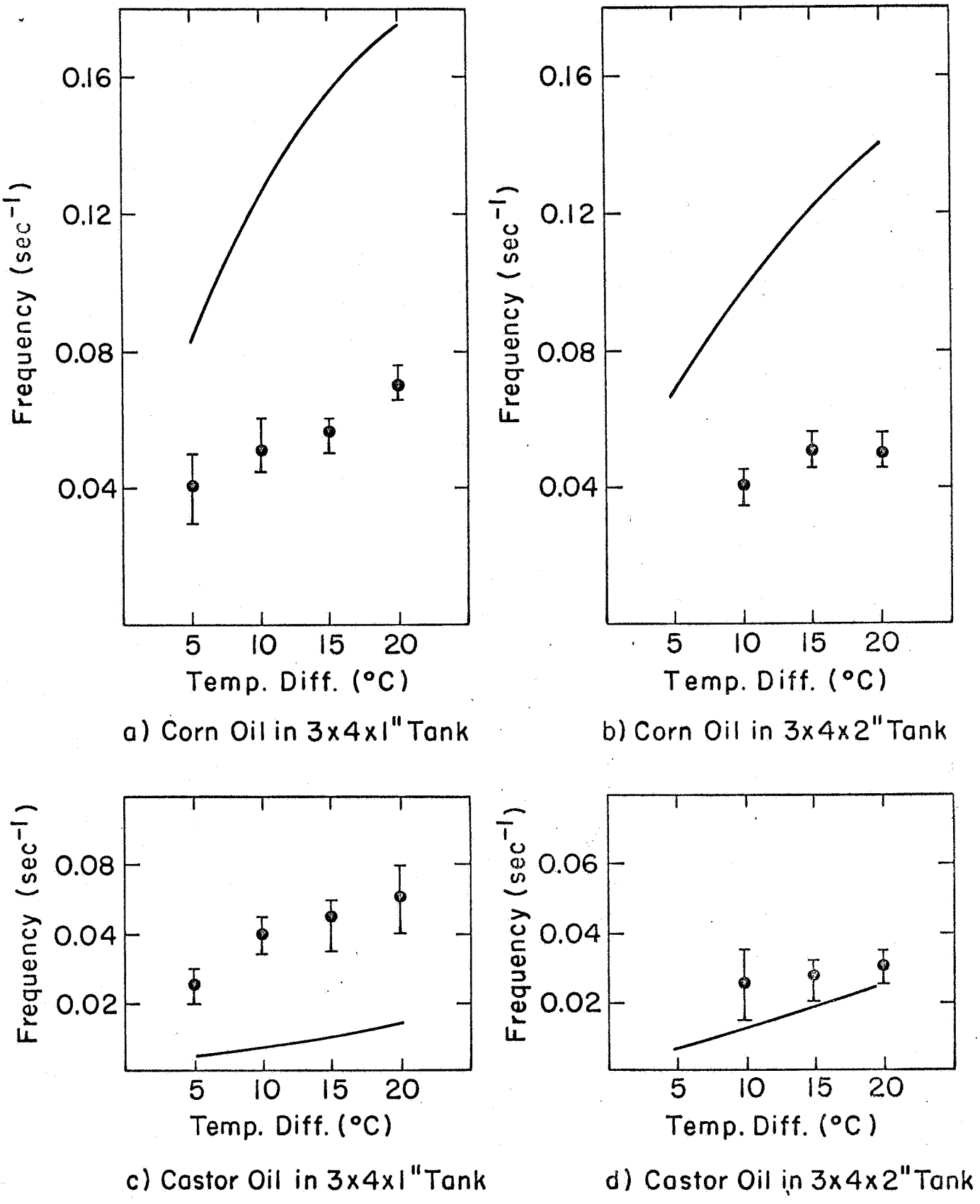

Fig. 10 Frequencies of the first unstable mode

threshold for instability, the system had a definite resonance with a large response. The resonance was fairly broad, with a width about equal to the center frequency. When the system was being excited at or near resonance, the sinusoidal steady-state response looked qualitatively the same as the onset of instability observed without the excitation, except in the immediate vicinity of the plate. The lines of constant phase were at an angle to the vertical and the phases traveled from top to bottom. Since driving the system at resonance probably meant exciting the first unstable mode, these results confirm that the unstable modes had phases that always traveled downward.

The resonant frequencies were the same as the frequencies measured previously using the phototube. Therefore, the discrepancy between theory and experiment really exists. The most plausible explanation for this discrepancy is that it occurs because the boundary conditions were not satisfied exactly. The frequencies depend very strongly on the wavenumber and therefore the boundaries play a very important role in determining the frequencies. Also, considering the approximations made in developing the theory, it may be that agreement within a factor of 2 or 3 is as good as could be expected.

III. HEAT TRANSFER USING ELECTRIC FIELDS

A. Experiments

Another method of detecting the onset of instability is to use

the Schmidt-Milverton principle.[17] The heat transfer across a tank with a known temperature gradient is measured and the Nusselt number calculated

$$Nu = \frac{Q}{(k\Delta T/d)} \qquad (1)$$

Q is the actual heat flow and $k\Delta T/d$ is the heat flow in the absence of convection. If the Nusselt number is greater than 1, convection is present. The apparatus used for the heat transfer experiments was that described in Section II-A except that a sheet of plate glass was placed between the bottom electrode and the low temperature bath. The desired temperature gradient was established and the voltage applied. After a steady-state temperature distribution was reached, the temperature drop across the test tank and the plate glass was measured. Since the thermal resistance of the plate glass was known the Nusselt number could be calculated.

The experimental data is shown in Figures 11 and 12. In these Figures the Nusselt number is plotted versus the electric field number, H.[1] Since the instability depends on several dimensionless numbers, no one single curve of Nu vs.H is possible. However for a given fluid and tank size the threshold value of H is a weak function of the temperature gradient. Therefore Figures 11 and 12 are plotted for a single fluid and test tank. The data then falls close to a single curve. The heat transfer data for corn oil shows a threshold slightly lower than that measured by visual detection indicating that the

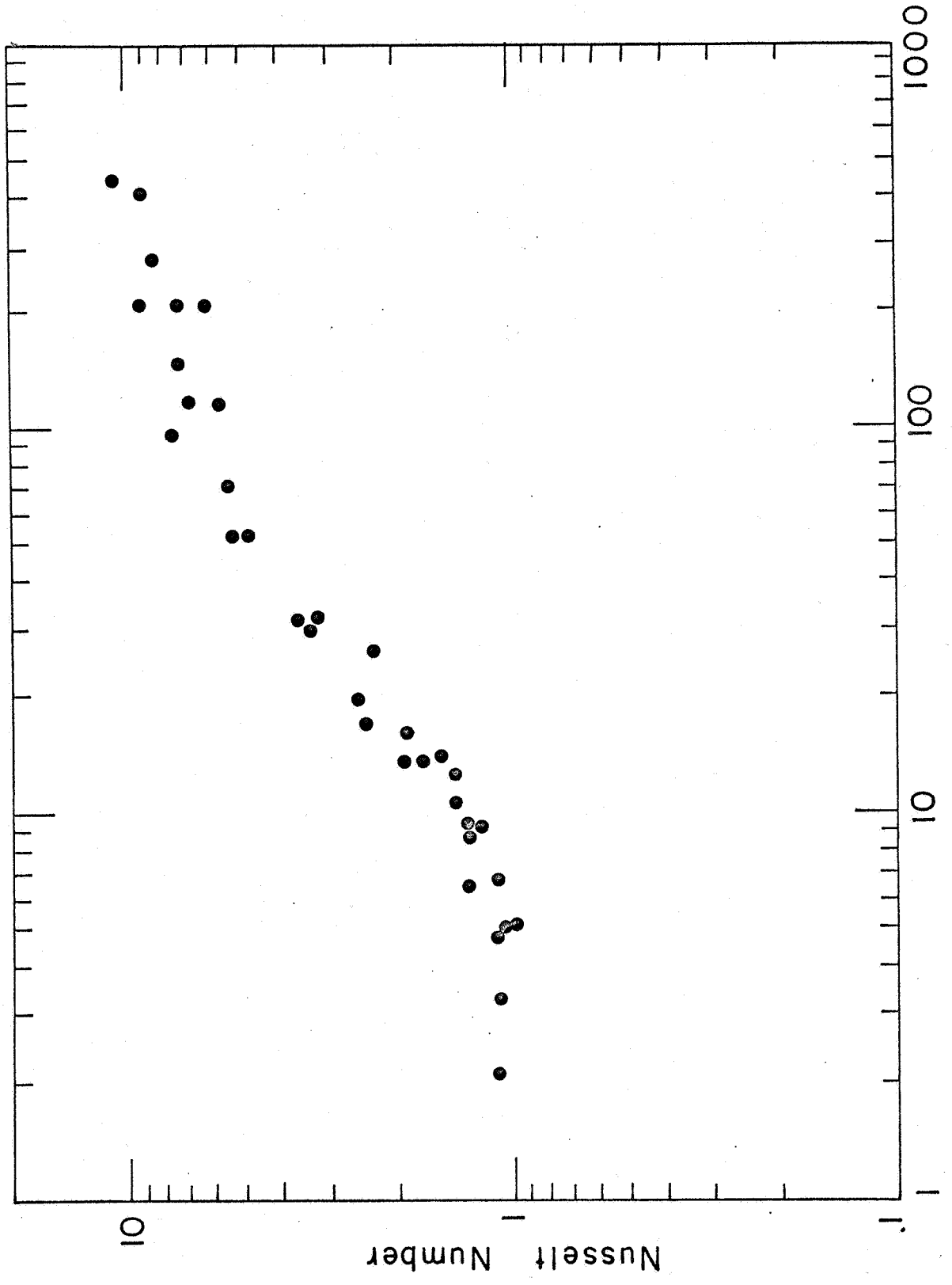

Fig. 11 Heat transfer data for corn oil in an electric field. The Nusselt number is one (no convection) until H (proportional to the voltage squarex) reaches the threshold for instability and then increases up to about 10 when the voltage reaches the breakdown strength of air. The test tank has dimensions 3" x 4" x 1".

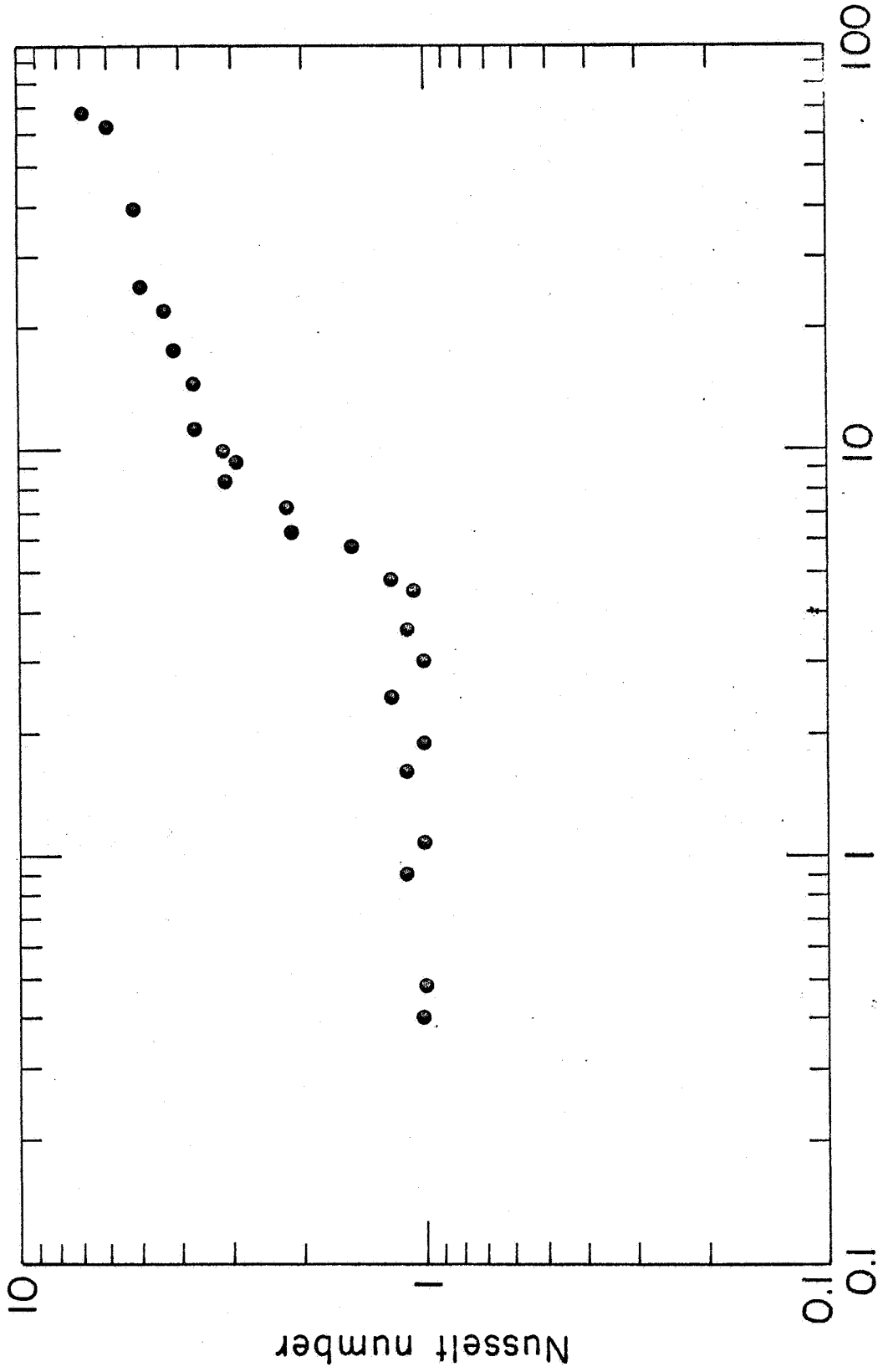

Fig. 12 Heat transfer data for castor oil in an electric field.
Same comments as for Fig. 11.

threshold in those experiments may have been overshot. For corn oil increasing H by a factor of 50 above threshold gives a tenfold increase in the heat transfer. Castor oil shows an increase of 500% with an H ten times the threshold value. The data used in Figures 11 and 12 is given in reference 18.

B. Consequences for Previous Work

In some of the papers on heat transfer in electric fields mentioned in the introduction the experimental data was correlated using the following theory.[7] The Nusselt number for heat transfer was assumed to have the form

$$Nu = f(Gr \cdot Pr) + g(El \cdot Pr) \tag{2}$$

where

$$Gr = \frac{\rho g d^3 \frac{d\rho}{dT} \Delta T}{\mu^2} \tag{3}$$

is the Grashof number,

$$Pr = \frac{c_p \mu}{k} \tag{4}$$

is the Prandtl number, and

$$El = \frac{\rho d^2 \Delta T E^2 \frac{d\varepsilon}{dT}}{\mu^2} \tag{5}$$

is a dimensionless electric field number introduced by Kronig and Schwarz.[7]

In the previously mentioned papers, researchers were correlating results with both a.c. and d.c. fields in both liquids and gases using the electric field number given in equation (5). This was done in spite of the fact that the forces produced by d.c. fields are often dominated by free charge effects while the similarity theory contains the assumption that the only electrical forces are those due to the gradient in dielectric constant. For problems where natural convection occurs, free charge effects are important whenever the electrical relaxation time is of the same order or less than the time needed for the fluid to traverse the space between the electrodes.

When the relaxation time is small, free charge forces will dominate the electric field effects and since the fractional change in conductivity is much greater than that of the dielectric constant, $\nabla\varepsilon$ may be neglected.[1] Thus for these cases $-1/2\ \mathbf{E}\cdot\mathbf{E}\nabla\varepsilon$ has been replaced by $\rho_f \mathbf{E}$ as the dominant electrical force term. The dimensionless number to replace El is found as follows

$$\left| \frac{\bar{\mathbf{E}}\cdot\bar{\mathbf{E}}\nabla\varepsilon}{\rho_f \mathbf{E}} \right| \sim \frac{|\nabla\varepsilon|}{\varepsilon} \frac{E}{\nabla\cdot\mathbf{E}} \tag{6}$$

But for smaller relaxation times

$$\nabla\cdot\sigma\mathbf{E} = 0 \tag{7}$$

$$\nabla\cdot\mathbf{E} = -\frac{\mathbf{E}\cdot\nabla\sigma}{\sigma} \tag{8}$$

$$\left| \frac{\bar{\mathbf{E}}\cdot\bar{\mathbf{E}}\nabla\varepsilon}{\rho_f \mathbf{E}} \right| \sim \frac{\sigma}{\varepsilon} \frac{|\nabla\varepsilon|}{|\nabla\sigma|} \sim \frac{\sigma}{\varepsilon} \frac{\frac{d\varepsilon}{dT}}{\frac{d\sigma}{dT}} \tag{9}$$

Therefore $d\epsilon/dT$ should be replaced in El by $\frac{\epsilon}{\sigma}\, d\sigma/dT$ and the new electric field number is

$$El' = \frac{\rho d^2 \nabla T \epsilon E^2 \frac{1}{\sigma}\frac{d\sigma}{dT}}{\mu^2} \qquad (10)$$

Examining El' shows why researchers have been able to correlate d.c. data with El. If the dielectric constant and conductivity are both assumed to be linear functions of temperature, the temperature gradient and electric field dependences of El and El' are identical. Any data that can be correlated using one may be correlated using the other, at least for a single fluid. Also $\frac{\sigma}{\epsilon}\ \frac{d\epsilon}{dT}/\frac{d\sigma}{dT}$ may not vary much for different liquids, and therefore El and El' give the same results. The difference between a.c. and d.c. results is accounted for by the difference between free charge and dielectric forces.

IV. CONCLUDING REMARKS

The experimental results presented in this paper show that the theory developed in Reference 1 correctly predicts the onset of instability for the class of problems considered. For poorly conducting fluids with temperature gradients the electroconvective instability is caused by free charge resulting from the conductivity gradients and dielectric forces may be neglected for d.c. fields.

ACKNOWLEDGMENTS

This paper is based on a thesis submitted to the Massachusetts Institute of Technology in partial fulfillment of the requirements for the degree of Doctor of Philosophy. The author wishes to acknowledge the help of Professor J. R. Melcher, his thesis supervisor. The work was supported by NASA under grant NsG-368.

REFERENCES

1) R. J. Turnbull, (Part I). (Of this paper.)

2) H. Senftleben, Phys. Z., 32, 550 (1931).

3) H. Senftleben, Phys. Z., 33, 826 (1932).

4) H. Senftleben, Phys. Z., 35, 661 (1934).

5) H. Senftleben, Z. Phys., 74, 757 (1932).

6) H. Senftleben and W. Braun, Z. Phys., 102, 480 (1936).

7) R. Kronig and N. Schwarz, Appl. Sci. Res., A1, 35 (1949).

8) G. Ahsmann and R. Kronig, Appl. Sci. Res., A2, 235 (1950).

9) H. DeHann, Appl. Sci. Res., A3, 85 (1951).

10) K. Weber and G. Halsey, Heat Transfer and Fluid Mechanics Institute, No. 19, University of Southern California, 1953.

11) E. Schmidt and M. Leidenfrost, Fors. Geb. Ing., 19, 65 (1953).

12) P. Watson, Nature, 189, 563 (1961).

13) P. Allen, Brit. J. Appl. Phys., 10, 347 (1959).

14) J. Coulsen and J. Porter, Trans I.C.E., 44, T388 (1966).

15) M. Cross and J. Porter, Nature, 212, 1343 (1964).

16) R. J. Turnbull, op. cit., equations 35 and 41.

17) R. J. Schmidt and S. W. Milverton, Proc. Roy. Soc. (London), A152, 586 (1935).

18) R. J. Turnbull, Ph.D. Thesis, Massachusetts Institute of Technology, (1967).

FIGURE CAPTIONS

1) Experimental Apparatus

2) Schlieren Pictures of the Instability

   a) No voltage

   b) Voltage less than the threshold for instability

   c) Voltage equal to the threshold value

   d) Voltage twice the threshold value

3) Shadowgraph pictures showing the moving phases. The pictures were taken five seconds apart. The bright line in the upper left hand corner of picture 1 moves down and to the right and then breaks up in picture 3. Picture 4 is very similar to picture 1 showing that the waves have a period of about 15 sec.

4) Fluid motions illustrated by a particle placed in the corn oil. The particle indicated by the arrow rises between pictures 1 and 2 before the wave front (bright line) passes. After the wave front has passed the particle goes down (pictures 3 and 4). The pictures are taken two seconds apart.

5) Voltage for instability for Corn oil in a one inch high tank as a function of the temperature difference. The bottom is maintained at 25^{o} C. The lines are theoretical curves with the dots and error brackets experimental data. The theoretical curves are calculated using the equations of reference 1.

6) Voltage for instability for corn oil in a two inch high tank. Same comments as for Figure 5.

7) Voltage for instability for castor oil in a one inch high tank. The bottom is maintained at 20^{o} C.

Figure Captions (continued)

8) Voltage for instability for castor oil in a two inch high tank with a bottom temperature of 20^{o} C.

9) Fluid properties as functions of temperature.

   a) Viscosity of corn oil

   b) Viscosity of castor oil

   c) Conductivity of corn oil

   d) Conductivity of castor oil

10) Frequencies of the first unstable mode.

   a) Corn oil in 3" x 4" x 1" tank with a bottom temperature of 25^{o} C.

   b) Corn oil in 3" x 4" x 2" tank with a bottom temperature of 25^{o} C.

   c) Castor oil in a 3" x 4" x 1" tank with a bottom temperature of 20^{o} C.

   d) Castor oil in a 3" x 4" x 2" tank with a bottom temperature of 20^{o} C.

11) Heat transfer data for corn oil in an electric field. The Nusselt number is one (no convection) until H (proportional to the voltage squared) reaches the threshold for instability and then increases up to about 10 when the voltage reaches the breakdown strength of air. The test tank has dimensions 3" x 4" x 1".

12) Heat transfer data for castor oil in an electric field. Same comments as for Figure 11.